ARTICLE

OPEN

Check for updates

Nucleation of jet engine oil vapours is a large source of aviation-related ultrafine particles

Florian Ungeheuer [1], Lucía Caudillo[1], Florian Ditas [2], Mario Simon[1], Dominik van Pinxteren[3], Doğuşhan Kılıç[4,5], Diana Rose[2], Stefan Jacobi[2], Andreas Kürten[1], Joachim Curtius [1] & Alexander L. Vogel [1✉]

Large airports are a major source of ultrafine particles, which spread across densely populated residential areas, affecting air quality and human health. Jet engine lubrication oils are detectable in aviation-related ultrafine particles, however, their role in particle formation and growth remains unclear. Here we show the volatility and new-particle-formation ability of a common synthetic jet oil, and the quantified oil fraction in ambient ultrafine particles downwind of Frankfurt International Airport, Germany. We find that the oil mass fraction is largest in the smallest particles (10-18 nm) with 21% on average. Combining ambient particle-phase concentration and volatility of the jet oil compounds, we determine a lower-limit saturation ratio larger than 1×10^5 for ultra-low volatility organic compounds. This indicates that the oil is an efficient nucleation agent. Our results demonstrate that jet oil nucleation is an important mechanism that can explain the abundant observations of high number concentrations of non-refractory ultrafine particles near airports.

[1] Institute for Atmospheric and Environmental Sciences, Goethe-University Frankfurt, Frankfurt am Main 60438, Germany. [2] Department for Ambient Air Quality, Hessian Agency for Nature Conservation, Environment and Geology, Wiesbaden 65203, Germany. [3] Atmospheric Chemistry Department (ACD), Leibniz Institute for Tropospheric Research (TROPOS), Leipzig 04318, Germany. [4] The Department of Earth and Environmental Sciences, the Faculty of Science and Engineering, the University of Manchester, Manchester M13 9PS, UK. [5] National Centre for Atmospheric Science, Manchester M13 9PS, UK. ✉email: vogel@iau.uni-frankfurt.de

Several studies identified airports as a major source of ultrafine particles (UFPs)[1–8]. Among different engine operation conditions at the airports, take-off is often associated with the highest UFP emissions[3,9–12]. These particles are typically formed via gas-to-particle conversion after combustion[13]. Transmission electron microscopy analysis of UFPs from aviation shows spherical particles with a volatile character under high vacuum[14]. They can be transported large distances from the source reaching densely populated residential areas, as large airports are usually located in the close vicinity of metropolitan areas[3,15,16]. UFP emissions from airport operations lead to a higher ambient particle number concentration (PNC) in the surrounding of airports, with a limited knowledge of their chemical composition[17,18]. UFP transport and subsequent infiltration to the indoor environment seems to be more relevant than infiltration of $PM_{2.5}$ and PM_{10}[18,19]. The number-size distributions of particles emitted by jet engines are dominated by a mode diameter smaller than ~30 nm, which is significantly smaller compared to particles from road traffic emissions[12,20–23]. Jet engine oil constituents (Supplementary Fig. 1) have been identified in UFPs near airports[2,7,24–26]. Lubrication oils are emitted from aircraft engines through a breather vent and unintentionally as leaks of the oil circulating system (i.e., due to worn seals)[24].

Due to the small size of UFPs, exposure-related health effects are of importance as they potentially reach the alveoli, penetrate through the pulmonary epithelium in the lower respiratory tract, and translocate the air-blood barrier[27–30]. Animal tests also showed that they can reach the central nervous system via the olfactory nerve circumventing the blood-brain barrier[31]. UFPs can permeate into the respiratory and cardiovascular system within minutes to hours and are still detectable for months after the exposure[32]. Depending on their chemical composition, UFPs can induce oxidative stress, inflammatory reactions, and cell membrane damages[33–35]. Health effects depend on their particle size, mass and number concentration[5], and additionally on individual properties such as surface area, solubility, oxidative potential and the ability to counteract macrophage phagocytosis[36]. Several studies investigated the UFP exposure of airport ground personnel and passengers[37,38] and health effects due to UFP exposure near the airport[6]. A recent cohort study reported a 12% increased risk of developing a malignant brain tumour in the Los Angeles airport area for each increase of UFP exposure by 6,700 particles cm^{-3}[39]. This finding is supported by a study from Toronto, which reports a hazard ratio of 1.112 in developing a malignant brain tumour per UFP increase of 10,000 particles cm^{-3}, adjusted for other air pollutants and sociodemographic factors[40]. A study of the health effects from long-term UFP exposure of airport workers reported no association to cardiovascular disease[41].

Ultrafine and fine particle emissions by jet engines during flight have also been investigated[42,43]. Here the focus has been put on determining emission indices for particle emissions at cruise and their role for contrail and cirrus formation[44]. Black carbon (soot) emissions have been discussed to dominate the formation of ice crystals in contrails, especially in the soot-rich regime characterised by soot particle number emission indices, EIs, in excess of ~10^{14} (kg-fuel)$^{-1}$[44]. Recent studies have shown that soot formation by aircraft engines burning plant-based bio-fuels blended with petroleum-based conventional kerosene (Jet A) or blends of synthetic fuels (Fischer-Tropsch) with Jet A fuel, both significantly reduces the soot formation[43,45], which is likely explained by the near zero aromatic contents of the bio and synthetic fuels. Ultrafine volatile particles were assumed to be mostly composed of sulphuric acid and organic fuel components that nucleate in the young exhaust plume[46,47], but jet lubrication oil has so far not been suggested as an important source of the freshly formed particles in the exhaust plume in flight.

In our previous study on airport-related UFPs, we showed that jet engine lubrication oils dominate the spectrum of detected organic compounds after a non-target analysis[26]. Following this non-target study, here we describe the nucleation ability of jet oil vapours in laboratory experiments and by quantification of jet engine oil constituents in three ambient UFP size fractions (<56 nm) downwind Frankfurt International Airport.

Results

Volatility and new-particle formation of jet engine lubrication oil. We compared particle-number size distributions (PNSD) of ambient UFPs with laboratory-generated jet oil particles. In the ambient measurements at Frankfurt-Schwanheim (Supplementary Fig. 2) we observe a distinct difference between UFPs from the airport and the city centre (Fig. 1a). Air masses transported from Frankfurt Airport show a ~15-times higher PNC of UFPs at ~18 nm compared to air masses from the city centre (wind roses are shown in Supplementary Fig. 3). For larger UFPs, this difference becomes less pronounced. In the laboratory, we studied the PNSD of atomised lubrication oil passing a thermodenuder at 20 °C and 300 °C to investigate the volatility and nucleation capability of the jet oil compounds. When the jet oil particles (mean diameter of 27 nm) pass the thermodenuder at 300 °C, we observe a more than fivefold increase of the particle number concentration compared to the experiment at 20 °C, and a reduction of the mean diameter
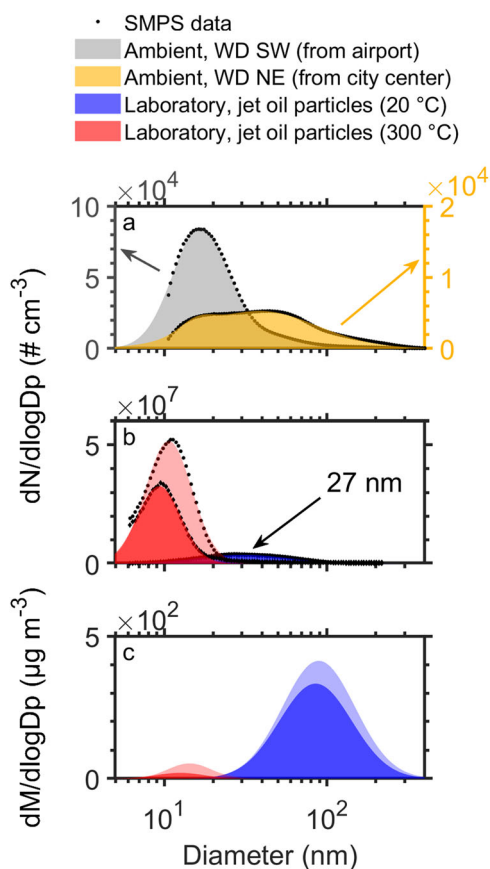
Fig. 1 Particle size distributions of ambient and laboratory-generated ultrafine particles. Ambient particle size distribution (**a**) at the monitoring site during wind direction (WD) from the airport (grey) and the city (yellow), averaged over three days (05:00–23:00 CET). Number-size (**b**) and mass-size distribution (**c**) from two laboratory experiments, each with jet oil nanoparticles generated from a methanolic solution, native at 20 °C (blue & light blue) and after heating to 300 °C (red & light red). Measurement data (black dots) were fitted using a lognormal distribution.

down to ~10 nm of the measured particles (Fig. 1b). Although the particles passed the thermodenuder, it is important to mention that the PNSD measurement was conducted downstream the heating section at room temperature. The volatility of the jet oil at 300 °C is evident as the mass fraction of jet oil is reduced by ~99% compared to the 20 °C control experiment (Fig. 1c). Downstream the heating section of the thermodenuder the majority of oil vapours in the gas phase is likely lost to the surfaces of the tubing. However, a small fraction of the oil vapours nucleates and forms new particles downstream of the thermodenuder within a few seconds, when the temperature of the sampling flow reaches a point at which the oil vapour becomes supersaturated. Rapid growth of particles to sizes >10 nm allows escaping the "valley of death" in the nucleation mode[48], in which small particles are efficiently scavenged by coagulation. The thermodenuder experiment demonstrates that jet engine oil particles are volatile UFPs at 300 °C, and it can be assumed that the oil partitions entirely to the gas phase if exposed to operating temperatures of aircraft turbofan engines (»300 °C[49]).

Fraction of lubrication oil in ambient UFP samples. We quantified jet engine oil constituents (Supplementary Fig. 1 and Supplementary Note 1) from ambient particle samples to determine the oil fraction in UFPs near Frankfurt Airport. Therefore, we collected UFP samples downwind the airport at Frankfurt-Schwanheim when air masses arrived from the airport (Fig. 2a–d). Using a cascade impactor (Nano-MOUDI), we sampled UFPs during seven periods (18–54 h) in three different UFP size bins (10–18 nm, 18–32 nm, 32–56 nm) for subsequent chemical analysis. From the continuous measurements of the PNSD we calculated the mass concentration (oil density = 1 g cm^{-3}, see Durdina et al.[50]) for the three investigated particle size bins (Fig. 2b–d). The corresponding UFP number concentration is shown in Supplementary Fig. 4. Particle mass concentration of the two smallest size bins (<32 nm) increased significantly (two-tailed t-test, $p < 0.001$) when the wind direction falls within the airport sector during its operating hours, compared to periods of other wind directions or non-operating hours. The variability of larger UFPs (>32 nm) does not show this behaviour (Fig. 2d–g). This is in accordance with previous studies, which state that the mode diameter of aircraft-related particle emissions is smaller than 30 nm, while the mode diameter of particles from on-road vehicles is predominantly larger than 30 nm[3,12,22,23]. The particle number concentration (<32 nm) reaches the rural background level around midnight. Hence, we consider the night-time periods between 00:00–05:00 CET adjacent to each sampling day as the mean rural background particle mass concentration that is largely unaffected by UFPs from the airport (dark red bars in Fig. 2b–d). Subtraction of the mean background mass from the mass during UFP sampling results in the total accumulated UFP mass on each impactor stage that can be attributed to the airport (Supplementary Figure 5 & Supplementary Table 1). This approach of mass closure cannot be applied to the largest stage (32–56 nm), because the particle mass concentration reaches sometimes higher values during non-operating than during operating hours (Fig. 2d).

We quantified the jet oil concentration of the individual impactor stages by adding authentic standards to aliquots of the filter extracts (standard addition method). Furthermore, we corrected for particle losses in the Nano-MOUDI based on an experimentally determined loss function of the three nano-stages (see Methods section). We find that jet engine oils contribute on average 21 ± 11% to the UFP mass in the 10–18 nm size bin. The jet-oil mass fraction of individual samples in the 10–18 nm size bin varies between 10 and 38%, with generally higher values for short sampling intervals. The contribution of jet engine oil to the total mass of the 18–32 nm particles is only 5 ± 3% on average

(Error estimation see Supplementary Note 2). Because the background subtraction could not be applied on the largest stage, we used the non-background corrected SMPS mass of the 32–56 nm stage and find a mean of 9% for the oil fraction of this size bin. Hence, the smallest particle stage shows consistently the highest mass fraction of jet engine lubrications oils (Supplementary Table 1 and Supplementary Fig. 6).

The calculation of the fractional oil contribution on all three stages did take into account experimentally determined particle losses. Regarding evaporative losses, we observe a bias in the molecular composition of jet oil from the ambient samples, which can be well explained by evaporation of the semi-volatile additives during Nano-MOUDI sampling (Supplementary Table 2). We evaluated the sampling efficiency of the Nano-MOUDI toward semi-volatiles based on pure ethyl oleate UFPs ($C_{20}H_{38}O_2$, 98%, Sigma-Aldrich) from an atomised solution. Although the generated PNSD covered the whole Nano-MOUDI range, we only detected the compound on the 32–56 nm stage (with the lowest pressure difference of the three Nano-MOUDI stages), and even on this stage we observed a loss of >99% of mass of the ethyl-oleate-UFPs. The vapour pressure of ethyl oleate is 8.10×10^{-3} Pa (EPI Suite[51]), which is similar to the vapour pressure of the N-phenyl-1-naphthylamine jet oil additive. The other additives and the jet oil esters exhibit lower vapour pressures (Supplementary Table 2). Therefore, it can be stated that the vapour pressure, and with this regard the volatilisation of semi-volatile compounds is the most important sampling loss process in the Nano-MOUDI. Fortunately, the jet oil esters are extremely low-volatile, and therefore evaporation of this compound class during sampling is negligible.

Lubrication oil base stock esters in the volatility basis set. The observed new-particle formation downstream the thermodenuder and the largest mass fraction of lubrication oil in the smallest ambient UFPs suggests that lubrication oil emissions from jet engines play a pivotal role in nucleation and early growth of new particles. We further evaluated this hypothesis by classifying the oils' synthetic esters into the volatility basis set (VBS[52–54]). Figure 3a shows the quantified ambient particle-phase concentration of single esters from two different jet oil base stocks: pentaerythritol esters ($C_{27-38}H_{48-70}O_8$) and trimethylolpropane esters ($C_{27-34}H_{50-64}O_6$). We used the SIM-POL.1 model[55] to estimate the vapour pressures of the different esters. We then calculated their saturation mass concentration C_i^* (at 293.15 K), which is the inverse of the gas-to-particle partitioning constant [Eq. 1], and assigned them to volatility classes[56]. In the ambient UFP samples, we measured particle-phase concentrations of the esters between 0.01 and 4 ng m^{-3}. Following, we calculated the theoretical gas-phase concentration, assuming that the esters' partitioning would shift entirely to the gas phase at ambient temperatures [Eq. 2]. As the lubrication oil concentration is not corrected for atmospheric dilution between the airport and the measurement station at Frankfurt-Schwanheim, the gas-phase concentration in the engine exhaust plumes at high temperatures (>300 °C) is certainly higher than this lower-limit estimate downwind of the airport. However, we still observe a large saturation ratio of the theoretical gas-phase concentration [Eq. 3], which we derived from ambient particle-phase concentrations (Fig. 3b). The three largest pentaerythritol esters, which fall into the region of ultra-low volatility, reach a saturation ratio of up to 3×10^5. Although this calculation is a lower-limit estimate, it supports the hypothesis that the synthetic esters from lubrication oils can initiate rapid nucleation in the exhaust plume of aircraft engines. Based on the theoretical gas-phase concentration, we
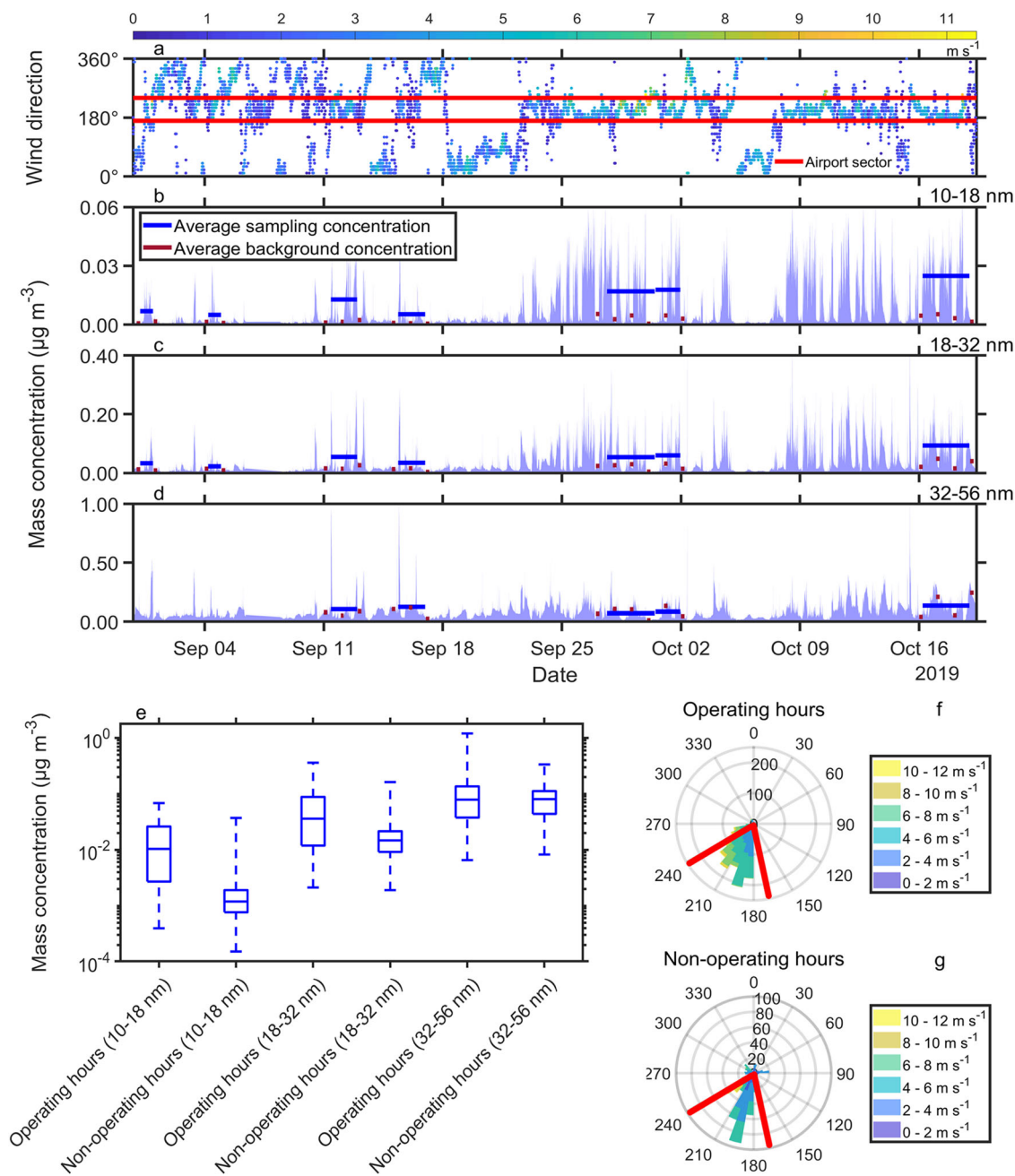
Fig. 2 Overview of the UFP mass concentrations derived from PNSD measurements and wind direction at Frankfurt Airport. Wind direction (**a**) with wind speed indicated by the colour code. The wind data is provided by the meteorological station at Frankfurt Airport (International Civil Aviation Organization, ICAO, code: EDDF) of the German weather service (DWD). The ambient UFP mass concentration (μg m^{-3}) in the size ranges 10–18 nm (**b**), 18–32 nm (**c**) and 32–56 nm (**d**), and the Nano-MOUDI sampling intervals (horizontal lines), indicating the average mass concentration during sampling hours (blue) and the average background mass concentration (dark red). Boxplots in (**e**) show the spread of the total mass concentrations (μg m^{-3}) for 10–18 nm, 18–32 nm and 32–56 nm particles during airport operating- and non-operating hours (based on SMPS data of the sampling- and background correction periods). The bottom and top of the boxes indicate the interquartile range and the horizontal line inside the boxes indicates the median. The whiskers show the scatter towards the most extreme values. The wind roses depict the prevailing wind directions during filter sampling at airport operating hours (**f**). Furthermore, the wind directions during the non-operating hour periods used for SMPS background correction are shown (**g**).

also determined the temperature at which each single ester compound reaches gas-phase supersaturation ($S_i^* > 1$) during cool-down of the exhaust plume [Eq. 6] (Fig. 3c). At ~60 °C, the ultra-low volatility pentaerythritol esters ($C_{36}H_{66}O_8$–$C_{38}H_{70}O_8$) are the first compounds that reach $S_i^* > 1$, although their ambient concentration is an order of magnitude lower than the extremely-low volatility ester $C_{29}H_{52}O_8$. Based on our measurements we observe that all synthetic esters reach

supersaturation at ambient temperature, except the three most volatile trimethylolpropane esters $C_{27-29}H_{50-54}O_6$.

Discussion

We interpret our laboratory thermodenuder experiment in such way that heated oil particles from an atomised solution generate gaseous oil vapours, which nucleate and form new ~10 nm
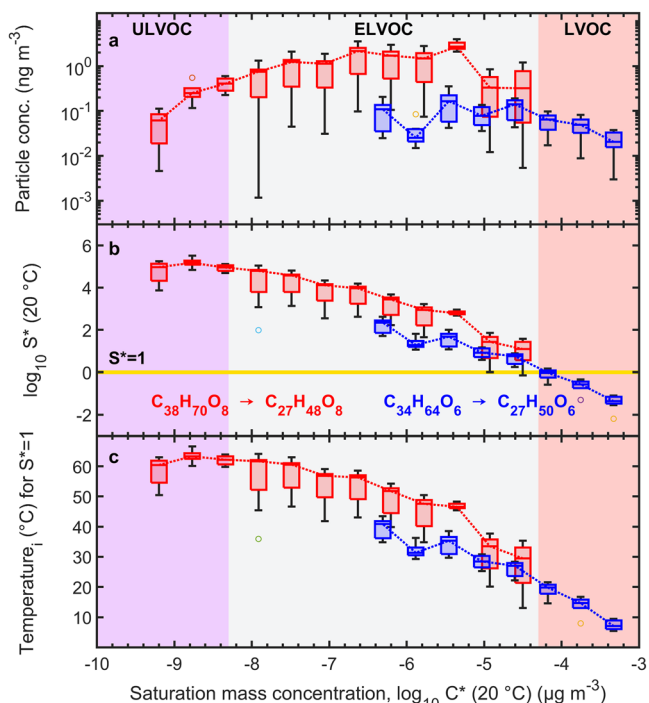
Fig. 3 Ambient concentrations of jet oil esters in the volatility basis set. **a** Quantified ambient particle concentration (ng m^{-3}) of each synthetic ester compound ($C_{27-38}H_{48-70}O_8$ (red boxes); $C_{27-34}H_{50-64}O_6$ (blue boxes)) plotted against the $\log_{10} C_i^*$ at 20 °C (ULVOC: ultra-low volatility-, ELVOC: extremely-low volatility-, LVOC: low-volatility organic compound). The boxes show the spread of the quantified mass concentrations (10–56 nm) as interquartile range during airport operating hours. The horizontal line within the boxes shows the median and the whiskers show the spread to the most extreme values. Values outside ±2.7 σ are marked as outliers by "o" symbols. **b** Resulting gas-phase saturation ratio S_i^* (20 °C) of the theoretical gas-phase concentration when all particle-phase compounds of (**a**) would partition to the gas phase. Values of S_i^* (20 °C) above 1 (yellow line) indicate supersaturation. **c** The approximate temperature at which the different jet oil esters reach $S_i^* = 1$.

particles right behind the heated section. This experiment demonstrates that the jet oil compounds are volatile at 300 °C, but also efficient nucleators at room or ambient temperature. The particle diameter of the freshly nucleated particles in our laboratory experiment appears in the same size region as the ambient UFPs downwind of Frankfurt Airport. Certainly, these laboratory experiments do not reflect the full complexity of jet engine emissions in the atmosphere. In real emission plumes, non-volatile particulate matter (nvPM) could scavenge nucleation by providing surface for condensation of oil vapours. However, earlier studies describe aviation-related UFPs as volatile under high vacuum[14], therefore, it appears likely that a large number of these particles, which are observed downwind of airports[12,23], are formed via nucleation of gaseous jet oil emissions.

Efficient nucleation and growth by organic compounds requires both (ultra-low) volatility compounds and sufficient high gas-phase concentrations for growing the particles fast enough. The lower concentration of the three ultra-low volatility organic compounds (ULVOCs) and higher concentrations of extremely-low volatility organic compounds (ELVOCs) create ideal conditions for initial nucleation by the jet oil ULVOCs, followed by rapid growth due to condensation from a large gas-phase reservoir of jet oil ELVOCs. The range of critical temperatures at which the compounds reach supersaturation suggests that nucleation and particle growth occurs in the near-field during

cool down of hot exhaust behind the turbofan (Fig. 4), and can explain the large volatile fraction (at elevated temperatures) of UFPs from aviation. To which extent the emission of nvPM from turbofan engines can scavenge this nucleation and growth needs further evaluation.

In fact, the reduction of nvPM emissions (e.g. soot) from aircraft engines in the last decades[57]—and with this the reduction of the condensational sink—might have led to an increase of the number concentration of volatile UFPs that are formed via nucleation of gaseous oil vapours or sulphuric acid. Nevertheless, the determined high gas-phase saturation ratios of the ULVOC synthetic esters suggest that nucleation can occur despite the presence of the condensation sink from nvPM. The dynamics of formation and condensation of semi-volatile oxidation products (e.g. from incomplete combustion) are not investigated in this study, but are complementary for understanding the UFP composition. Hence, the above-mentioned Nano-MOUDI sampling artefacts are critical, as low- and semi-volatile oxidation products, which can contribute to UFP mass, are lost during sampling. Despite these uncertainties and considering that our results are lower-limit estimates, they substantiate the main finding that jet-oil vapours reach gas-phase supersaturation in cooling emission plumes leading to rapid nucleation and formation of UFPs in the range of ~10–20 nm.

Our observations of lubrication oil emissions being an important source for UFPs implies that this source will not be addressed by replacing traditional jet fuels with sustainable aviation fuels (SAF)[45], and should therefore also be taken into account in the current endeavour to eliminate UFP emissions from aviation. Accordingly, the air/oil separator should be optimised with regard to an improved jet oil recovery, and thus preventing oil emissions. In addition, developing advanced maintenance routines and reducing the total uptime of jet engines at airports (e.g. through electrification of ground handling) could also reduce oil emissions. Furthermore, evaluation of the toxicological properties of jet oil UFPs should be conducted to assess their health effects, also considering detrimental and potentially neurotoxic substances that are either directly emitted (e.g. organophosphates as lubrication oil additives[58,59]), or which are formed through thermal transformation of the utilised trimethylolpropane esters (e.g. trimethlyolpropane phosphate)[26,60]. Furthermore, lubricant oil emissions during cruise and their possible effects on cirrus cloud formation needs further investigation, as the oil effect (e.g. as an organic coating on soot particles) has not been studied, yet.

Materials and methods

Jet engine oil thermodenuder measurements. We used thermodenuder measurements to determine the volatility of jet oil UFPs, as the new international aircraft particulate matter standard only considers the number and mass concentration of nvPM[61]. We determined the particle-number size distribution of Mobil Jet^{TM} Oil II UFPs, formed using an atomizer (replica of TSI model 3076) with 0.04 g L^{-1} jet oil solved in ultra-pure methanol. The resulting PNSD downstream of the thermodenuder (operated at 20 °C and 300 °C) was measured using a scanning-mobility particle sizer (SMPS, TSI, model: 3938, Shoreview, MN, USA). The remaining jet engine oil fraction after the heating section was determined by comparing the particle mass derived from the PNSD measurements at both temperatures.

Impactor sampling and molecular characterisation. Detailed information on sampling technique, sample preparation and extraction procedure can be found elsewhere[26]. Briefly, we used a Micro Orifice Uniform Deposition Impactor (Nano-MOUDI, Model 115, MSP, Minneapolis, MN, USA) at an air-quality monitoring site in Frankfurt-Schwanheim and sampled particles on the three nano-stages <56 nm. All stages were equipped with aluminium foils (TSI, diameter 47 mm and thickness 0.015 mm), and the upper ten stages were coated with Apiezon® grease to minimise the bounce-off of larger particles.

In the period of August to October 2019, we sampled UFPs for 18–54 h during airport operating hours (5:00–23:00 CET) and during southerly wind direction.
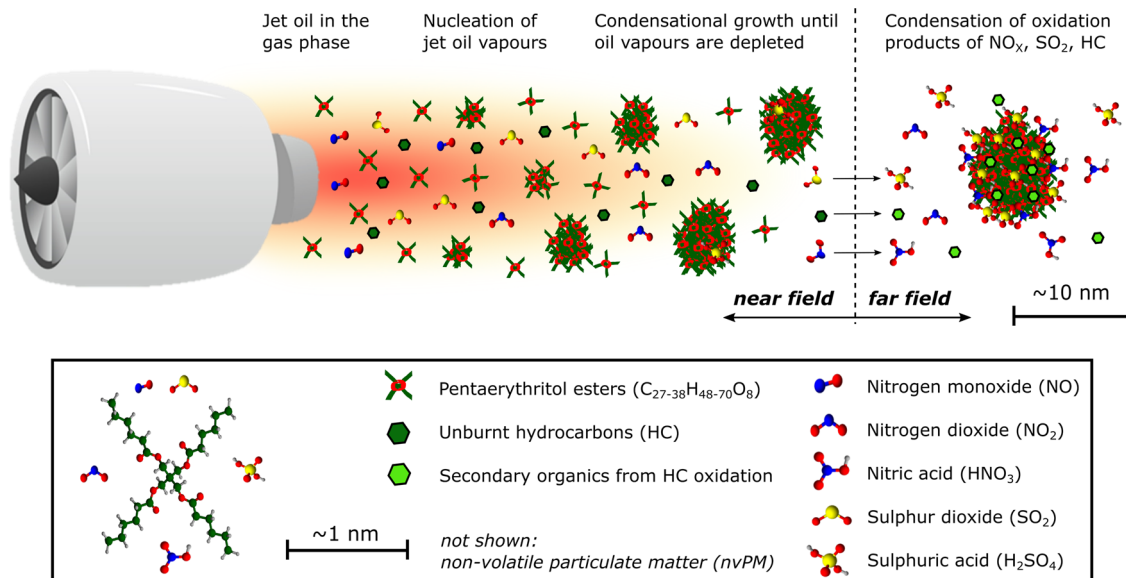
Fig. 4 Conceptual illustration of the UFP formation. Emissions of aircraft turbofan engines result in fast nucleation and growth of jet oil vapours in the near field. Non-volatile emissions (nvPM) are not shown. Dimensions are not true to scale.

Without an active sampling airflow, we collected field blanks for 115 h on the three nano-stages to estimate possible background concentrations regarding the target compounds. We stored the filters until analysis at −20 °C. Due to the extensive sampling time span, we assume that our UFP samples represent aircraft engines of several types under various operating states. This is essential for covering the average UFP emission of the whole airport and not of individual engines or certain engine operating states.

We quantified the additives and jet oil esters using standard addition with authentic and surrogate standards, respectively (Supplementary Figs. 7 and 8). Targeted measurements of the jet engine oil constituents were carried out by using ultra-high performance liquid chromatography (UHPLC)/heated electrospray ionisation (HESI) coupled to an Orbitrap high-resolution mass spectrometer (HRMS). Chromatographic separation of the jet engine oil constituents was accomplished using a C_{18}-reversed phase column (Details see Supplementary Note 3). Using the standard addition method, we quantified 23 compounds in 25 ambient filter samples including 3 blank samples (Details see Supplementary Note 4). Most of these compounds belong to the group of pentaerythritol- or trimethylolpropane esters, which are utilised as jet engine oil base stocks (Supplementary Table 2). Finally, we determined the jet engine oil mass of the deposited UFPs after field blank correction.

Experimental loss determination in the Nano-MOUDI. Since sampling UFPs with a Nano-MOUDI is accompanied by particle losses, we determined a loss factor for each Nano-MOUDI stage (Details see Supplementary Note 5, Supplementary Figs. 9–11, and Supplementary Table 3). The loss of particles with an aerodynamic diameter between 32–56 nm is 28% and for 18–32 nm particles 40%, respectively. We were not able to experimentally determine a loss factor for the smallest size bin of 10–18 nm particles, due to insufficient deposited mass. We calculated the loss under the assumption that particle diffusivity is the main driving force for sampling losses of extremely low-volatile compounds in the UFP size range. We determined the dependency between particle diameter and diffusion coefficient at 17.2 kPa and 20 °C (sampling condition of the 18–32 nm stage). To fit the experimentally determined particle losses of the two larger stages, we applied a damping term on the diffusion coefficient equation (Supplementary Fig. 11). Based on the experimentally determined losses of the two upper nano-stages, we calculated a loss of ~58% for the smallest stage. This loss factor can be considered as a conservative estimate, as it is only based on particle diffusive losses and not including losses due to evaporation after impaction (see main text). By implementing these loss factors, we corrected the quantified jet oil filter mass and determined the mass fraction of jet engine lubrication oils in airport-related UFPs.

Ambient SMPS measurements. The PNSD at the sampling site was determined using a SMPS including an electrostatic classifier (TSI, model: 3082), a Differential Mobility Analyser (DMA, TSI, model: 3081) and a Condensation Particle Counter (CPC, TSI, model: 3772). Ambient air was sampled through a stainless-steel tube (inner diameter: 20 mm, length 1.6 m), using a $PM_{2.5}$ inlet head at a flow rate of 1 $m^3\,h^{-1}$. Prior entering the SMPS, the aerosol passes a Nafion dryer (1.2 m length, flow rate of 0.3 $m^3\,h^{-1}$) to stabilise the relative humidity below 40%. The actual sample flow of the SMPS was 1 $L\,min^{-1}$, the additional bypass is used to minimise

residence time and particle losses in the inlet system. The PNSD was measured in the size range of 10–500 nm at a temporal resolution of 5 min. Particle losses due to sedimentation, inertial impaction and diffusion have been calculated and corrected accordingly[62]. The UFP mass was determined by integration assuming spherical particles. We calculated the particle mass for each filter collection interval exclusively during airport operating hours by converting the PNSD into a volume distribution averaged over the sampling period using a unit density of 1 $g\,cm^{-3}$ and the Nano-MOUDI sampling flow rate of 0.6 $m^3\,h^{-1}$. The particle density was chosen according to the analysed jet engine oil densities (see safety data sheets) and aircraft turbine engine studies[50]. Consequently, conversion of the measured mobility diameter to aerodynamic diameter is not necessary[63]. We analysed the SMPS data of seven filter sampling periods as no data is available for one sampling period due to an instrument failure.

Volatility and saturation ratio of jet oil esters. The volatility of compounds strongly determines their gas-to-particle partitioning behaviour. Hence, evaluation of the jet oil base stocks using semi-empirical group contribution methods (SIM-POL.1 model[55]) and the volatility basis set (VBS[52,53]) enables the grouping of the single ester compounds to volatility classes (ULVOC: ultra-low volatility-, ELVOC: extremely-low volatility-, LVOC: low-volatility organic compound). Compound classification is based on their volatility expressed as the logarithm of the saturation mass concentration ($\log_{10} C_i^*$), where the volatility is differentiated by one decade in C_i^*, which is also assumed as uncertainty. The saturation mass concentration (C_i^* (µg m^{-3})) is calculated as the inverse of the gas-to-particle phase partitioning constant (K_p)[52] taking into account the weight fraction of the absorbing organic material (om) phase (f_{om}), its average molecular weight (MW_{om}, g mol^{-1}), and the activity coefficient (ζ_i) and vapour pressure ($p_{L,i}^0$, Torr)[52,64] of compound i:

$$\frac{1}{\zeta_i * C_i^*} = K_p = \frac{f_{om} * 760 * R * T}{MW_{om} * \zeta_i * p_{L,i}^0 * 10^6} \quad (1)$$

We calculated K_p assuming the absorbing organic phase consists only of the respective substance ($f_{om} = 1$), which leads to an ideal absorption affinity of the molecules passing from the gas phase to the particle phase ($\zeta_i = 1$). The compound's affinity to the particle phase inversely correlates with ζ_i[65]. R is the gas constant (8.2×10^{-5} m^3 atm mol^{-1} K^{-1}) and T (K) the temperature.

We converted the quantified base stock ester concentrations in the particle phase ($\frac{m_i}{V}$ (g m^{-3})) to gas phase number concentrations (c_i^v (m^{-3})) using the ideal gas law (m_i: quantified ester mass; M_i: molecular mass in g mol^{-1}):

$$c_i^v = \frac{m_i * N_A}{V * M_i} \quad (2)$$

To determine whether jet oil constituents reach gas-phase supersaturation, we calculated their gas-phase saturation ratio (S_i^*)[66]:

$$S_i^* = \frac{c_i^v * M_i * 10^6}{C_i^* * N_A} \quad (3)$$

Accounting for the temperature dependence of the saturation vapour pressure, C_i^* can be described according to the Clausius-Clapeyron equation:

$$\log_{10} C_i^*(T) = \log_{10} C_i^*(293.15\,\text{K}) + \frac{\Delta H_i^{vap}}{R * \ln(10)} * \left(\frac{1}{293.15\,\text{K}} - \frac{1}{T} \right) \quad (4)$$

where $R = 8.314 \times 10^{-3}\,\text{kJ}\,\text{K}^{-1}\,\text{mol}^{-1}$. The evaporation enthalpy ΔH_i^{vap} (kJ mol^{-1}) can be approximated by:

$$\Delta H_i^{vap} = -11 * \log_{10} C_i^*(293.15\,\text{K}) + 129 \quad (5)$$

Despite the large uncertainties of this approach[67], it still can be used to describe a simple estimate of the temperature dependence of the oil partitioning. Finally, we combined [Eq. 3] and [Eq. 4] to calculate the approximate temperature at which the jet oil esters reach gas-phase supersaturation ($S_i^* = 1$) in a cooling engine exhaust plume [Eq. 6].

$$T_i^{S^*=1} = -\frac{1}{\log_{10}\left(\frac{c_i^j * M_i * 10^6}{N_A * C_i^*(293.15\,\text{K})}\right) * \frac{R * \ln(10)}{\Delta H_i^{vap}} - \frac{1}{293.15\,\text{K}}} \quad (6)$$

Reporting summary. Further information on research design is available in the Nature Portfolio Reporting Summary linked to this article.

Data availability

References

1. Hu, S. et al. Aircraft emission impacts in a neighborhood adjacent to a general aviation airport in southern California. *Environ. Sci. Technol.* **43**, 8039–8045 (2009).
2. Yu, Z. et al. Identification of lubrication oil in the particulate matter emissions from engine exhaust of in-service commercial aircraft. *Environ. Sci. Technol.* **46**, 9630–9637 (2012).
3. Keuken, M. P., Moerman, M., Zandveld, P., Henzing, J. S. & Hoek, G. Total and size-resolved particle number and black carbon concentrations in urban areas near Schiphol airport (the Netherlands). *Atmos. Environ.* **104**, 132–142 (2015).
4. Stafoggia, M. et al. Particle number concentrations near the Rome-Ciampino city airport. *Atmos. Environ.* **147**, 264–273 (2016).
5. Yu, Z. et al. Evaluation of PM emissions from two in-service gas turbine general aviation aircraft engines. *Atmos. Environ.* **160**, 9–18 (2017).
6. Habre, R. et al. Short-term effects of airport-associated ultrafine particle exposure on lung function and inflammation in adults with asthma. *Environ. Int.* **118**, 48–59 (2018).
7. Fushimi, A., Saitoh, K., Fujitani, Y. & Takegawa, N. Identification of jet lubrication oil as a major component of aircraft exhaust nanoparticles. *Atmos. Chem. Phys.* **19**, 6389–6399 (2019).
8. Rivas, I. et al. Source apportionment of particle number size distribution in urban background and traffic stations in four European cities. *Environ. Int.* **135**, 105345 (2020).
9. Zhu, Y., Fanning, E., Yu, R. C., Zhang, Q. & Froines, J. R. Aircraft emissions and local air quality impacts from takeoff activities at a large International Airport. *Atmos. Environ.* **45**, 6526–6533 (2011).
10. Hsu, H.-H. et al. The relationship between aviation activities and ultrafine particulate matter concentrations near a mid-sized airport. *Atmos. Environ.* **50**, 328–337 (2012).
11. Hsu, H.-H. et al. Contributions of aircraft arrivals and departures to ultrafine particle counts near Los Angeles International Airport. *Sci. Total Environ.* **444**, 347–355 (2013).
12. Pirhadi, M. et al. Relative contributions of a major international airport activities and other urban sources to the particle number concentrations (PNCs) at a nearby monitoring site. *Environ. Pollut.* **260**, 114027 (2020).
13. Pekkanen, J. & Kulmala, M. Exposure assessment of ultrafine particles in epidemiologic time-series studies. *Scand. J. Work Environ. Health* **30**, 9–18 (2004).
14. Mazaheri, M., Bostrom, T. E., Johnson, G. R. & Morawska, L. Composition and morphology of particle emissions from in-use aircraft during takeoff and landing. *Environ. Sci. Technol.* **47**, 5235–5242 (2013).
15. Hudda, N. & Fruin, S. A. International airport impacts to air quality: size and related properties of large increases in ultrafine particle number concentrations. *Environ. Sci. Technol.* **50**, 3362–3370 (2016).
16. Zhang, X., Karl, M., Zhang, L. & Wang, J. Influence of aviation emission on the particle number concentration near zurich airport. *Environ. Sci. Technol.* **54**, 14161–14171 (2020).
17. Hudda, N., Simon, M. C., Zamore, W. & Durant, J. L. Aviation-related impacts on ultrafine particle number concentrations outside and inside residences near an airport. *Environ. Sci. Technol.* **52**, 1765–1772 (2018).
18. Hudda, N., Durant, L. W., Fruin, S. A. & Durant, J. L. Impacts of aviation emissions on near-airport residential air quality. *Environ. Sci. Technol.* **54**, 8580–8588 (2020).
19. Chen, C. et al. Outdoor-to-indoor transport of ultrafine particles: measurement and model development of infiltration factor. *Environ. Pollut.* **267**, 115402 (2020).
20. Riley, E. A. et al. Ultrafine particle size as a tracer for aircraft turbine emissions. *Atmos. Environ.* **139**, 20–29 (2016).
21. Masiol, M., Harrison, R. M., Vu, T. V. & Beddows, D. C. S. Sources of sub-micrometre particles near a major international airport. *Atmos. Chem. Phys.* **17**, 12379–12403 (2017).
22. Shirmohammadi, F. et al. Emission rates of particle number, mass and black carbon by the Los Angeles International Airport (LAX) and its impact on air quality in Los Angeles. *Atmos. Environ.* **151**, 82–93 (2017).
23. Stacey, B. Measurement of ultrafine particles at airports: a review. *Atmos. Environ.* **198**, 463–477 (2019).
24. Yu, Z. et al. Characterization of lubrication oil emissions from aircraft engines. *Environ. Sci. Technol.* **44**, 9530–9534 (2010).
25. Timko, M. T. et al. Particulate emissions of gas turbine engine combustion of a fischer−tropsch synthetic fuel. *Energy Fuel.* **24**, 5883–5896 (2010).
26. Ungeheuer, F., van Pinxteren, D. & Vogel, A. L. Identification and source attribution of organic compounds in ultrafine particles near Frankfurt International Airport. *Atmos. Chem. Phys.* **21**, 3763–3775 (2021).
27. Oberdörster, G. et al. Extrapulmonary translocation of ultrafine carbon particles following whole-body inhalation exposure of rats. *J. Toxicol. Environ. Health Part A* **65**, 1531–1543 (2002).
28. Oberdörster, G., Oberdörster, E. & Oberdörster, J. Nanotoxicology: an emerging discipline evolving from studies of ultrafine particles. *Environ. Health. Persp.* **113**, 823–839 (2005).
29. Kreyling, W. G. et al. Air-blood barrier translocation of tracheally instilled gold nanoparticles inversely depends on particle size. *ACS Nano* **8**, 222–233 (2014).
30. Lu, D. et al. Chemical multi-fingerprinting of exogenous ultrafine particles in human serum and pleural effusion. *Nat. Commun.* **11**, 2567 (2020).
31. Oberdörster, G. et al. Translocation of inhaled ultrafine particles to the brain. *Inhal. Toxicol.* **16**, 437–445 (2004).
32. Miller, M. R. et al. Inhaled nanoparticles accumulate at sites of vascular disease. *ACS Nano* **11**, 4542–4552 (2017).
33. Nel, A., Xia, T., Mädler, L. & Li, N. Toxic potential of materials at the nanolevel. *Science* **311**, 622–627 (2006).
34. Jonsdottir, H. R. et al. Non-volatile particle emissions from aircraft turbine engines at ground-idle induce oxidative stress in bronchial cells. *Commun. Biol.* **2**, 90 (2019).
35. Ohlwein, S., Kappeler, R., Kutlar Joss, M., Künzli, N. & Hoffmann, B. Health effects of ultrafine particles: a systematic literature review update of epidemiological evidence. *Int. J. Public Health* **64**, 547–559 (2019).
36. Chalupa, D. C., Morrow, P. E., Oberdörster, G., Utell, M. J. & Frampton, M. W. Ultrafine particle deposition in subjects with asthma. *Environ. Health. Persp.* **112**, 879–882 (2004).
37. Møller, K. L. et al. Occupational exposure to ultrafine particles among airport employees-combining personal monitoring and global positioning system. *PLoS ONE* **9**, e106671 (2014).
38. Ren, J., Cao, X. & Liu, J. Impact of atmospheric particulate matter pollutants to IAQ of airport terminal buildings: a first field study at Tianjin Airport, China. *Atmos. Environ.* **179**, 222–226 (2018).
39. Wu, A. H. et al. Association between airport-related ultrafine particles and risk of malignant brain cancer: A Multiethnic Cohort Study. *Cancer Res.* **81**, 4360–4369 (2021).
40. Weichenthal, S. et al. Within-city spatial variations in ambient ultrafine particle concentrations and incident brain tumors in adults. *Epidemiology* **31**, 177–183 (2020).
41. Møller, K. L. et al. Cardiovascular disease and long-term occupational exposure to ultrafine particles: a cohort study of airport workers. *Int. J. Hyg. Environ. Health* **223**, 214–219 (2020).
42. Brock, C. A. et al. Ultrafine particle size distributions measured in aircraft exhaust plumes. *J. Geophys. Res.* **105**, 26555–26567 (2000).
43. Voigt, C. et al. Cleaner burning aviation fuels can reduce contrail cloudiness. *Commun. Earth. Environ.* https://doi.org/10.1038/s43247-021-00174-y (2021).

44. Kärcher, B., Burkhardt, U., Bier, A., Bock, L. & Ford, I. J. The microphysical pathway to contrail formation. *J. Geophys. Res. Atmos.* **120**, 7893–7927 (2015).

45. Moore, R. H. et al. Biofuel blending reduces particle emissions from aircraft engines at cruise conditions. *Nature* **543**, 411–415 (2017).

46. Anderson, B. E., Cofer, W. R., Barrick, J. D., Bagwell, D. R. & Hudgins, C. H. Airborne observations of aircraft aerosol emissions II: Factors controlling volatile particle production. *Geophys. Res. Lett.* **25**, 1693–1696 (1998).

47. Curtius, J. et al. First direct sulfuric acid detection in the exhaust plume of a jet aircraft in flight. *Geophys. Res. Lett.* **25**, 923–926 (1998).

48. Wang, M. et al. Rapid growth of new atmospheric particles by nitric acid and ammonia condensation. *Nature* **581**, 184–189 (2020).

49. El-Sayed, A. F. *Aircraft Propulsion And Gas Turbine Engines* (CRC Press Taylor & Francis Group, 2017).

50. Durdina, L. et al. Determination of PM mass emissions from an aircraft turbine engine using particle effective density. *Atmos. Environ.* **99**, 500–507 (2014).

51. United States Environmental Protection Agency. *US EPA. [2021]. Estimation Programs Interface Suite™ v 4.11* (Washington, DC, USA, 2012).

52. Donahue, N. M., Robinson, A. L., Stanier, C. O. & Pandis, S. N. Coupled partitioning, dilution, and chemical aging of semivolatile organics. *Environ. Sci. Technol.* **40**, 2635–2643 (2006).

53. Donahue, N. M., Epstein, S. A., Pandis, S. N. & Robinson, A. L. A two-dimensional volatility basis set: 1. organic-aerosol mixing thermodynamics. *Atmos. Chem. Phys.* **11**, 3303–3318 (2011).

54. Donahue, N. M., Kroll, J. H., Pandis, S. N. & Robinson, A. L. A two-dimensional volatility basis set—Part 2: diagnostics of organic-aerosol evolution. *Atmos. Chem. Phys.* **12**, 615–634 (2012).

55. Pankow, J. F. & Asher, W. E. SIMPOL.1: a simple group contribution method for predicting vapor pressures and enthalpies of vaporization of multifunctional organic compounds. *Atmos. Chem. Phys.* **8**, 2773–2796 (2008).

56. Stolzenburg, D. et al. Rapid growth of organic aerosol nanoparticles over a wide tropospheric temperature range. *Proc. Natl. Acad. Sci. USA* **115**, 9122–9127 (2018).

57. Lee, D. S. et al. Transport impacts on atmosphere and climate: aviation. *Atmos. Environ.* **44**, 4678–4734 (2010).

58. Duarte, D. J., Rutten, J. M. M., van den Berg, M. & Westerink, R. H. S. In vitro neurotoxic hazard characterization of different tricresyl phosphate (TCP) isomers and mixtures. *Neurotoxicology* **59**, 222–230 (2017).

59. Hageman, G., Mackenzie Ross, S. J., Nihom, J. & van der Laan, G. *Occupational Neurotoxicology*, edited by M. Aschner (Elsevier Science & Technology, San Diego, 2022), Vol. 7, p. 77–132.

60. Keefer, E. W., Gramowski, A., Stenger, D. A., Pancrazio, J. J. & Gross, G. W. Characterization of acute neurotoxic effects of trimethylolpropane phosphate via neuronal network biosensors. *Biosens. Bioelectron.* **16**, 513–525 (2001).

61. International Civil Aviation Organization (ICAO). *Environmental Report Aviation And Environment. Destination Green The Next Chapter. International Civil Aviation Organization (ICAO)* (2019).

62. Weiden, S.-L., von der, Drewnick, F. & Borrmann, S. Particle Loss Calculator —a new software tool for the assessment of the performance of aerosol inlet systems. *Atmos. Meas. Tech.* **2**, 479–494 (2009).

63. Seinfeld, J. H. & Pandis, S. N. *Atmospheric Chemistry and Physics. From Air Pollution to Climate Change*. 3rd ed. (Wiley, s.l., 2016).

64. Pankow, J. F. An absorption model of gas/particle partitioning of organic compounds in the atmosphere. *Atmos. Environ.* **28**, 185–188 (1994).

65. Williams, B. J., Goldstein, A. H., Kreisberg, N. M. & Hering, S. V. In situ measurements of gas/particle-phase transitions for atmospheric semivolatile organic compounds. *Proc. Natl. Acad. Sci. USA* **107**, 6676–6681 (2010).

66. Donahue, N. M. et al. How do organic vapors contribute to new-particle formation. *Faraday Discuss.* **165**, 91–104 (2013).

67. Epstein, S. A., Riipinen, I. & Donahue, N. M. A semiempirical correlation between enthalpy of vaporization and saturation concentration for organic aerosol. *Environ. Sci. Technol.* **44**, 743–748 (2010).

Author contributions

F.U. wrote the paper; designed research, performed the field sampling, sample preparation, measurements, lab experiments and majority of data analysis; L.C. performed lab experiments and analysed data; F.D. and D.R. performed SMPS measurements; M.S., D.v.P., S.J., D.K., A.K. and J.C. advised on data interpretation; A.L.V. designed research, advised on data analysis, data interpretation and manuscript writing; edited and revised the manuscript; and directed the project administration. All authors commented on the manuscript and contributed to the scientific discussion.

Competing interests

The authors declare no competing interests.

Additional information

Supplementary information The online version contains supplementary material available at https://doi.org/10.1038/s43247-022-00653-w.

Correspondence and requests for materials should be addressed to Alexander L. Vogel.

Peer review information *Communications Earth & Environment* thanks the anonymous reviewers for their contribution to the peer review of this work. Primary Handling Editors: Clare Davis. The peer reviewer reports are only from the second round of peer-review.

Reprints and permission information is available at http://www.nature.com/reprints

Publisher's note Springer Nature remains neutral with regard to jurisdictional claims in published maps and institutional affiliations.